T Lymphocyte Activation Threshold and Membrane Reorganization Perturbations in Unique Culture Model

CL Adams and CF Sams

Life Sciences Research Laboratories, NASA - Johnson Space Center, Houston, TX 77058, USA

Quantitative activation thresholds and cellular membrane reorganization are mechanisms by which resting T cells modulate their response to activating stimuli. Here we demonstrate perturbations of these cellular processes in a unique culture system that non-invasively inhibits T lymphocyte activation. During clinorotation, the T cell activation threshold is increased 5-fold. This increased threshold involves a mechanism independent of TCR triggering. Recruitment of lipid rafts to the activation site is impaired during clinorotation but does occur with increased stimulation. This study describes a situation in which an individual cell senses a change in its physical environment and alters its cell biological behavior.

Quantitative activation thresholds determine the activation response of peripheral T lymphocytes. Different activation stimuli vary in their potency, and the actual response of a T cell depends on ligand density[1,2], ligand binding affinity[3,4], and the state of the T cell[5,6]. T cells internalize their receptors (TCRs) following ligation and activate when a critical threshold of TCR triggering has been reached, irrespective of the nature of the stimulating ligand[7]. This threshold level of TCR stimulation necessary for activation can be modulated, however, by other factors such as costimulation. Costimulation through CD28 lowers the threshold for T cell activation to one-fifth the number of triggered TCRs necessary for stimulation through CD3 alone[7].

Ligation of CD28 during T cell activation initiates a reorganization of cellular membrane structures by recruiting specialized membrane microdomains to the contact site[8]. These movable domains, termed lipid rafts, are composed primarily of sphingolipids and cholesterol. Lipid rafts are also enriched with GPI-linked proteins and several signal transduction molecules including lck and fyn[9] and are proposed to function as preformed platforms for signal transduction[10]. Recruitment of lipid rafts to the contact site may provide a cellular mechanism by which the T cell can amplify TCR-mediated signals and lower the threshold for activation.

Reduced gravity cell culture provides a unique opportunity to study pathways mediating T cell activation. Clinorotation provides a functionally weightless environment by counterbalancing the sedimentation rate of cells in suspension[11]. Even though gravity remains present, the gravitational vector is randomized and fluid shear is minimized as single cells rotate quasi-stationary with the culture media[12]. Many of the cellular changes observed during space flight also occur during clinorotation, including an inhibition of the T cell activation response to mitogenic signals[13]. Specifically, peripheral blood mononuclear cells stimulated with lectins or monoclonal antibodies show a dramatic reduction in T lymphocyte proliferation[14]. This inhibition occurs at an early stage of the activation process as surface expression of the early activation marker CD69 and the IL-2 Receptor (CD25) are also inhibited[15]. This inhibition does not occur when purified T cells are activated with phorbol ester plus ionomycin, suggesting an early block in signal transduction[15,16]. Phorbol ester, however, is a very potent activator and may overcome T cell inhibition by enhanced stimulation rather than bypassing a specific block in the signaling cascade.

Interestingly, activation of purified T cells during clinorotation can be achieved using polystyrene beads coated with antibodies to the TCR/CD3 complex and the costimulatory molecule CD28, despite the inability of these same antibodies to induce activation when presented on Antigen Presenting Cells (APCs)[15]. Since it is possible to bind more antibodies to a bead than an APC, we questioned whether the amount of stimulus was a more important factor in determining T cell activation in reduced gravity culture than the pathway of stimulation. In this study we demonstrate that an increased activation threshold underlies the non-invasive T cell inhibition induced by clinorotation. We further show that early cell biological processes associated with lymphocyte activation, namely membrane reorganization and cell spreading, are hampered in the reduced gravity environment of this cell culture model.

Results

Clinorotation increases activation threshold. To generate dose-response curves for activation of normal human peripheral T cells, polystyrene beads were titrated with increasing concentrations of anti-CD3/28 cocktail (anti-CD3 plus anti-CD28 monoclonals mixed at a 1:1 ratio) just prior to use. The density of anti-CD3/28 bound to the beads was determined by indirect immunofluorescence and used as the measure of stimulus dose (units). Cells stimulated during clinorotation show a dramatic right shift in the dose-response curves for expression of the early activation marker CD69 (Fig 1a), expression of the IL-2 receptor (CD25, Fig 1b), and entry into S phase (BrdU incorporation, Fig 1c).

Lower densities of anti-CD3/28 (2 - 5 units) induce full activation of static cultures but do not activate T cells during clinorotation (Figure 1, a-c). Increasing the density of antibody stimulation diminishes T cell inhibition during clinorotation. This is consistent with an increased activation threshold during clinorotation. The dose-response curves obtained for static activation show minimal variation from one experiment to the next. For a given amount of stimulation, the percent cells activated is highly reproducible, even for antibody densities that activate less than 80% of the cells (0 – 2 units). On the contrary, despite a highly consistent curve shift, the actual percent cells activated for a given density of antibody stimulation is highly variable during clinorotation. Increased variability in the level of activation during clinorotation likely reflects impaired signal integration rather than reduced levels of signaling.

Curve fit analysis. To quantitate the change in the activation threshold during clinorotation, we performed a least-squares curve fit analysis on the collected data. The T cell activation curves shown in Figure 1 display a saturation function. The sigmoidal shape indicates a greater than first order dependence on activator concentration. This can be empirically modeled using the equation

$$\%A = \%A_{max}[x^p/(K_m + x^p)]$$

where x is the antibody density on the bead and %A is the percentage of activated cells. $\%A_{max}$, K_m, and p are parameters of the system that are affected both by clinorotation and the complexity of the activation level measured. These values will thus vary between clinorotation and static culture and among different measurements of activation. $\%A_{max}$ is the maximum percent cells that can be activated assuming an infinite density of stimulating antibody. The empirical parameter p allows for greater than first order dependence on antibody density. Solving for K_m reveals that $(K_m)^{1/p}$ is the equivalent of x_{50}, the antibody density that produces half-maximal activation, or $K_m = (x_{50})^p$. Substitution gives

$$\%A = \%A_{max}[x^p/((x_{50})^p + x^p)]$$

This equation is equivalent to the Hill equation for sigmoid substrate saturation enzyme kinetics. Here it describes a simple sigmoidal saturation function for which the slope of the dose-response curve and the maximal level of activation can be modulated by the inhibitor (clinorotation).

Using this equation, we performed least squares analysis on cumulative data from the dose-response experiments. Curve fits are shown in Figure 2 with parameters of the equations and statistics listed in Table 1. Excellent curve fits were obtained for static activation curves using this equation (R-squared values of 0.99 or greater). Good fits were also obtained for CD69 (Fig 2a) and BrdU (Fig 2b) clinorotation curves, with lower R-squared values (0.91-0.94) reflecting the high variability in the level of activation for a given stimulus dose rather than a poor curve fit. Empirical $\%A_{max}$ values determined by the equation were consistent with the observed values. The average observed $\%A_{max}$ for CD69 expression is 71.76, within the 74.96 $\pm$ 5.90 predicted value. Likewise, the theoretical $\%A_{max}$ of 50.72 $\pm$ 4.53 for relative BrdU incorporation matches the observed average of 50.00. Since approximately 10% of unactivated peripheral T cells express CD25, the activation curve for CD25 is not accurately predicted by this equation, which assumes a basal expression of zero.

The antibody density necessary for half-maximal activation (x_{50}) during clinorotation was increased 5 fold above static values for both CD69 expression and relative BrdU incorporation (Table 1). Thus, clinorotation raises the threshold for T cell activation by the same order of magnitude that costimulation through CD28 lowers it. As we progress from expression of early activation markers to gene transcription and proliferation, the inhibitory effect of clinorotation is likely amplified and increasingly complex. This is manifested by the decrease in $\%A_{max}$ from CD69 expression to BrdU incorporation (Table 1).

TCR triggering not responsible. Since the dynamics of cell-cell and cell-bead encounters are different during clinorotation and static culture, several have argued that diminished T cell activation in during reduced gravity culture may simply be a reflection of decreased TCR stimulation. Valitutti et al have shown that TCR stimulation can be measured by CD3 internalization[17]. Following ligation of the TCR, the TCR/CD3 complex is internalized and the difference in expression with and without stimulation is a measurement of the level of TCR triggering. TCR down-regulation is induced by early events following specific engagement by an agonist and

can be dissociated from those required for full T cell activation[18]. Bachmann et al have shown that the degree of TCR down-regulation is a function of ligand affinity and titration, and the degree of down-regulation correlates with the T cell functional response to stimulation[19].

To assess the relationship between TCR triggering in the change of threshold, the level activation (measured by CD69 expression) was plotted as a function of TCR internalization (Fig 3). TCR internalization was measured by subtracting the mean channel fluorescence of FITC-labeled anti-CD3 binding to stimulated cells from unstimulated controls. Cumulative data from seven experiments are shown in Figure 3 and parameters for the curve fit analysis are listed in Table 1. A 2.4-fold increase in the amount of TCR triggering necessary for 50% activation indicates that a mechanism independent of TCR stimulation is involved in the increased threshold for T cell activation during reduced gravity culture. This demonstrates a deficit in T cell signal transduction and cannot be explained by differences in cell-cell or cell-bead interactions between static and reduced gravity cultures.

T cell activation experiments using anti-CD3 and anti-CD28 on polystyrene beads were previously performed in real microgravity during space shuttle missions STS-81 and STS-84[15]. Inhibition of T cell activation during space flight was greater than observed for clinorotation, suggesting, at the time, differences between true microgravity and ground-based models. The in-flight T cell activation experiments[15], however, did not measure the density of stimulating antibody on the bead at the time of activation. The affinity binding of mouse monoclonals to the GAM-coated beads is highly unstable and storage of the beads for as little as one week results in a dramatic decrease in the potency of the beads (unpublished observations). This is much more evident in reduced gravity culture for which activation is much more sensitive to subtle changes in the amount of stimulus. Storage time and vibration during launch may have significantly decreased the antibody density on the beads used for in-flight activation. When the activation results from STS-81 and STS-84 are expressed as a function of CD3 internalization, the data correlates with the curves shown in Figure 3.

Raft recruitment and cell spreading affected. Costimulation through CD28 during TCR ligation induces the redistribution of lipid rafts to the site of TCR engagement and lowers the threshold for T cell activation[8]. To determine if the dynamics of lipid raft recruitment following activation are compromised during clinorotation, we analyzed raft surface distribution using FITC-labeled cholera toxin (CTx) B subunit, which binds to the GM1 glycosphingolipid present in lipid rafts.

To correlate the competency of T cells to activate with the extent of lipid raft recruitment, we stimulated resting T cells with either "lo" or "hi" anti-CD3/28. In these experiments "lo" anti-CD3/28 (0.5 ug/ml, bead antibody density of 7.0 $\pm$ 0.45 units) yielded full activation of T cells (94.0 $\pm$ 1.07%) in static culture, with only partial activation (30.7 $\pm$ 7.23%) during clinorotation (Fig 4a). Stimulation with "hi" anti-CD3/28 (20ug/ml, density of 30 $\pm$ 1.91 units) increased the percentage of cells activated during clinorotation to 64.6 $\pm$ 7.72 % (Fig 4b).

Fluorescent microscopy of lo stimulated cells revealed that raft recruitment following activation is indeed impaired during clinorotation as is the ability of the cell to spread onto the bead (Figures 4 and 5). 85-90% of cells stimulated in static culture with either hi or lo anti-CD3/28 wrap around the bead and show intense staining of lipid rafts at the bead/cell contact site (Fig 4, Fig 5 a-f). On the contrary, cells stimulated with lo anti-CD3/28 during clinorotation attach to beads but remain rounded and do not spread (Fig 4a, 5g-i). 75% of cells do not exhibit any raft recruitment to the contact site although some cells demonstrate raft recruitment in the absence of spreading (Fig 5i). Cells stimulated with hi anti-CD3/28 during clinorotation do exhibit cell spreading and raft recruitment comparable to static culture (Fig 5k,l) but not as consistently (Fig 4b). This indicates that cells stimulated during clinorotation can indeed attach to and wrap around a bead and reorganize membrane microdomains. These processes are impaired during clinorotation but can be overcome by increasing the amount of stimulation. The percentage cells spreading and recruiting lipid rafts correlated well with the percentage of activated cells for both clinorotated and static cultures (Fig 4).

Discussion

The ability of an individual cell to sense and respond to changes in its chemical environment is well established (i.e., chemotaxis[20]). Similarly, it is easy to comprehend how multi-cellular systems interpret changes in the physical environment via integrin-mediated mechanotransduction[21]. The mechanism by which a single cell senses changes in its physical environment and alters its cell biological behavior, however, is poorly understood. The noninvasive inhibition of T cell activation afforded by clinorotation provides a unique opportunity to study not only the complex cellular events regulating T cell activation but also the effects of physical perturbation on cellular biological processes within individual cells.

The results of this study clearly indicate that T lymphocytes can indeed reorganize membrane structure,

change cell shape, express early activation markers, induce new gene expression and undergo proliferation in response to membrane-external activation stimuli during clinorotation, but the amount of stimulus necessary for this response is substantially higher than in static culture. Correlation of activation with TCR internalization (Fig 3) proves a deficit in signal transduction exists independent of TCR triggering that cannot be explained by diminished cell/bead interactions. Costimulation through CD28 and recruitment of lipid rafts to the contact site is intimately associated with the activation threshold[8]. It is uncertain whether impaired raft recruitment during clinorotation raises the activation threshold, or if signal transduction pathways upstream of membrane reorganization are affected by the increased threshold.

The cytoskeleton may provide the critical link between the physical environment and the diminished capacity of T lymphocytes to change cell shape and reorganize membrane structure during clinorotation. Don Ingber's work describes a tension-dependent architecture within living cells that involves all three cytoskeletal filament systems as well as nuclear scaffolds[22,23]. Alterations in this cellular force balance, known as tensegrity, influence intracellular biochemistry[24] and gene expression in the nucleus[25]. Disruption of internal cellular force balances in a microgravity environment[26] may compromise the ability of cells to properly integrate activation signals that require cytoskeletal and membrane reorganization.

Lymphoid cell spreading onto surface-immobilized antibodies requires active rearrangement of the cytoskeletal actin structure[27]. Movement of the actin cytoskeleton also mediates the translocation of lipid rafts to the contact site[28]. Space flight studies reveal microtubule organization in lymphoblastoid cells is impaired in microgravity culture[29], but further studies are required to determine the effects of microgravity and clinorotation on actin structure. Reorganization of cytoskeletal and membrane structures facilitates enhanced and sustained T cell signaling via spatial and temporal organization of the signaling machinery[30]. Diminished efficacy of these cell biological functions in reduced gravity culture would impair signal integration in T lymphocytes, increasing both the threshold and variability for activation, as reported here for clinorotation.

Methods

Bead preparation. Goat anti-mouse antibodies (Fc-specific, Sigma) were covalently bound to 6 micron carboxylated beads (latex microspheres) according to the protocol given by the supplier (Polysciences, Inc., Warrington PA). Just prior to use, increasing concentrations of anti-CD3(Orthoclone okt3, Orthobiotech, Raritan NJ) plus anti-CD28(Leu-28, Becton Dickinson, San Jose CA) mouse monoclonal antibodies were affinity bound to the goat anti-mouse beads for 3 hours at RT. Anti-CD3 and anti-CD28 were used at a 1:1 ratio and the amount of total antibody bound to each bead set was indirectly measured by flow cytometry as the mean channel fluorescence (MCF) of FITC-labeled Goat anti-mouse (polyclonal against the entire mouse antibody, Becton Dickinson).

Isolation of T cells. Peripheral blood mononuclear cells (PBMC's) were isolated from fresh human blood or buffy coat packs by standard Ficoll-Hypaque (Pharmacia Biotech, Uppsala, Sweden) density gradient centrifugation. Normal healthy donors were obtained through the NASA test subjects facility at Johnson Space Center and were prescreened for HIV and Hepatitis B. Pre-screened buffy coats were obtained from Gulf Coast Blood Center. T cells were purified from PBMC's using a Human T cell Enrichment Column (R&D Systems, Inc., Minneapolis MN) according to the protocol given by the supplier.

Activation and culture conditions. Purified T cells were suspended at a concentration of 1 million cells per ml in complete RPMI (RPMI 1640 supplemented with 10% fetal bovine serum, 100 units/ml Penicillin G, 100 ug/ml Streptomycin sulfate, and 2mM L-Glutamine). Each bead set was added at a 5 to 1 ratio of beads to cells and samples were immediately aliquoted into 1.2 ml cryovials (filled to capacity) and placed in clinorotation or static culture at 37C. Clinorotation was performed at 20 rpm about the longitudinal axis, with the axis of rotation perpendicular to the gravity vector. Cells were harvested at 48 hours for surface marker expression and cell proliferation measurements.

Measurement of cell surface expression. Harvested cells were immediately stained with FITC-conjugated anti-CD3 (Leu-4) plus PE-conjugated anti-CD69 (Leu-23), anti-CD25 (anti-IL-2-R), or mouse IgG1 isotype control (Becton Dickinson). Two-color flow cytometry to detect surface expression of CD3, CD69, and CD25 was performed using a Coulter Epics XL cytometer. Activation results are reported as the percentage of cells positive for the CD69 and CD25 surface markers relative to the mouse IgG control. Downregulation of TCR/CD3 was measured by indirect immunofluorescence on intact cells using antibodies to CD3 (FITC-Leu4). The level of TCR downregulation was estimated by the decrease in fluorescence intensity relative to unstimulated controls.

Measurement of cell proliferation. Harvested cells were pulsed for 2 hours with 5-bromo-2-deoxyuridine (BrdU, Sigma) and stained with anti-BrdU-FITC (Becton Dickinson) according to the protocol given by the supplier. The percentage of cells in S phase was determined by flow cytometry as the percentage of BrdU positive cells.

Curve fit analysis was performed by the least squares method using Stata software (Stata Corporation, College Station, Texas).

Cell image analysis. Purified T cells were suspended at a concentration of 2 million cells per ml in complete RPMI and stimulated with anti-CD3/28 beads at a 1:1 ratio for 1 hour during clinorotation or static culture. Cells were fixed in 3% formaldehyde/2 mM EGTA/PBS, stained with FITC-conjugated Cholera Toxin B (8 ug/ml, Sigma), and plated onto PEI coated slides. Scoring of cell/bead interactions for cell spreading and lipid raft recruitment was performed by fluorescent microscopy. One-hundred cell/bead interactions were scored for each sample for each of three independent experiments. Images were collected on a Zeiss LSM 410 laser scanning confocal microscope.

Acknowledgements

Funding for this investigation was provided by grants 121-10-90-13 and 199-93-17-13 from the National Aeronautics and Space Administration. CL Adams was supported by a National Research Council Resident Research Associateship at the Johnson Space Center and by the National Space Biomedical Research Institute. This investigation is part of a NASA Specialized Center of Research and Training collaboration between Rice University and the Johnson Space Center. Special Thanks to Al Feiveson for his assistance with curve fit analysis and statistics.

References

1. Motta, I., Lone, Y. C. & Kourilsky, P. In vitro induction of naive cytotoxic T lymphocytes with complexes of peptide and recombinant MHC class I molecules coated onto beads: role of TCR/ligand density. *Eur J Immunol* **28**, 3685-95 (1998).
2. Hemmer, B., Stefanova, I., Vergelli, M., Germain, R. N. & Martin, R. Relationships among TCR ligand potency, thresholds for effector function elicitation, and the quality of early signaling events in human T cells. *J Immunol* **160**, 5807-14 (1998).
3. Kwok, W. W., Reijonen, H., Falk, B. A., Koelle, D. M. & Nepom, G. T. Peptide binding affinity and pH variation establish functional thresholds for activation of HLA-DQ-restricted T cell recognition. *Hum Immunol* **60**, 619-26 (1999).
4. Bachmann, M. F. *et al.* T cell responses are governed by avidity and co-stimulatory thresholds. *Eur J Immunol* **26**, 2017-22 (1996).
5. Metz, D. P., Farber, D. L., Taylor, T. & Bottomly, K. Differential role of CTLA-4 in regulation of resting memory versus naive CD4 T cell activation. *J Immunol* **161**, 5855-61 (1998).
6. Waldrop, S. L., Davis, K. A., Maino, V. C. & Picker, L. J. Normal human CD4+ memory T cells display broad heterogeneity in their activation threshold for cytokine synthesis. *J Immunol* **161**, 5284-95 (1998).
7. Viola, A. & Lanzavecchia, A. T cell activation determined by T cell receptor number and tunable thresholds [see comments]. *Science* **273**, 104-6 (1996).
8. Viola, A., Schroeder, S., Sakakibara, Y. & Lanzavecchia, A. T lymphocyte costimulation mediated by reorganization of membrane microdomains [see comments]. *Science* **283**, 680-2 (1999).
9. Casey, P. J. Protein lipidation in cell signaling. *Science* **268**, 221-5 (1995).
10. Simons, K. & Ikonen, E. Functional rafts in cell membranes. *Nature* **387**, 569-72 (1997).
11. Klaus, D. M., Todd, P. & Schatz, A. Functional weightlessness during clinorotation of cell suspensions. *Adv. Space Res.* **21**, 1315-1318 (1998).
12. Unsworth, B. R. & Lelkes, P. I. Growing tissues in microgravity. *Nat Med* **4**, 901-7 (1998).
13. Cogoli, A. & Cogoli-Greuter, M. Activation and proliferation of lymphocytes and other mammalian cells in microgravity. *Adv Space Biol Med* **6**, 33-79 (1997).
14. Cogoli, A., Tschopp, A. & Fuchs-Bislin, P. Cell sensitivity to gravity. *Science* **225**, 228-30 (1984).
15. Hashemi, B. B. *et al.* T cell activation responses are differentially regulated during clinorotation and in spaceflight. *Faseb J* **13**, 2071-2082 (1999).
16. Cooper, D. & Pellis, N. R. Suppressed PHA activation of T lymphocytes in simulated microgravity is restored by direct activation of protein kinase C. *J Leukoc Biol* **63**, 550-62 (1998).
17. Valitutti, S., Muller, S., Cella, M., Padovan, E. & Lanzavecchia, A. Serial triggering of many T-cell receptors by a few peptide-MHC complexes [see comments]. *Nature* **375**, 148-51 (1995).
18. Salio, M., Valitutti, S. & Lanzavecchia, A. Agonist-induced T cell receptor down-regulation: molecular requirements and dissociation from T cell activation. *Eur J Immunol* **27**, 1769-73 (1997).
19. Bachmann, M. F. *et al.* Peptide-induced T cell receptor down-regulation on naive T cells predicts agonist/partial agonist properties and strictly correlates with T cell activation. *Eur J Immunol* **27**, 2195-203 (1997).
20. Armitage, J. P. Bacterial tactic responses. *Adv Microb Physiol* **41**, 229-89 (1999).
21. Duncan, R. L. & Turner, C. H. Mechanotransduction and the functional response of bone to mechanical strain. *Calcif Tissue Int* **57**, 344-58 (1995).
22. Wang, N., Butler, J. P. & Ingber, D. E. Mechanotransduction across the cell surface and through the cytoskeleton [see comments]. *Science* **260**, 1124-7 (1993).
23. Maniotis, A. J., Chen, C. S. & Ingber, D. E. Demonstration of mechanical connections between integrins, cytoskeletal filaments, and nucleoplasm that stabilize nuclear structure. *Proc Natl Acad Sci U S A* **94**, 849-54 (1997).
24. Chicurel, M. E., Chen, C. S. & Ingber, D. E. Cellular control lies in the balance of forces. *Curr Opin Cell Biol* **10**, 232-9 (1998).
25. Chen, C. S., Mrksich, M., Huang, S., Whitesides, G. M. & Ingber, D. E. Geometric control of cell life and death. *Science* **276**, 1425-8 (1997).
26. Ingber, D. How cells (might) sense microgravity. *Faseb J* **13**, S3-15 (1999).
27. Kim, J. H., Glant, T. T., Lesley, J., Hyman, R. & Mikecz, K. Adhesion of Lymphoid Cells to CD44-Specific Substrata: The Consequences of Attachment Depend on the Ligand. *Exp Cell Res* **256**, 445-453 (2000).
28. Wulfing, C. & Davis, M. M. A receptor/cytoskeletal movement triggered by

costimulation during T cell activation. *Science* **282**, 2266-9 (1998).

29. Lewis, M. L. *et al.* Spaceflight alters microtubules and increases apoptosis in human lymphocytes (Jurkat). *Faseb J* **12**, 1007-18 (1998).

30. Grakoui, A. *et al.* The immunological synapse: a molecular machine controlling T cell activation [see comments]. *Science* **285**, 221-7 (1999).

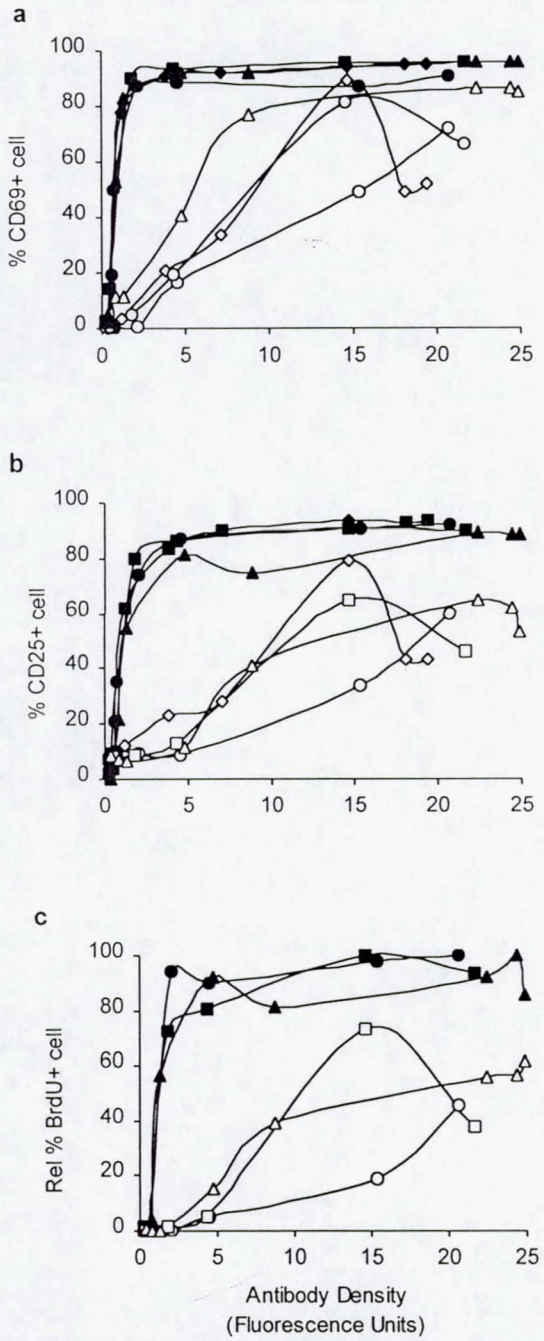

Figure 1 **Increased T cell activation threshold during clinorotation.** Dose-response curves for T cells stimulated by increasing densities of anti-CD3/28 (okt3+leu28) during clinorotation (open symbols) and static culture (closed symbols) for three (c) or four (a,b) independent experiments. The density of antibody used for stimulation (units) was measured by indirect immunofluorescence as the Mean Channel Fluorescence of FITC-labeled Goat anti-mouse binding to the antibody coated beads. Activation is expressed as the percent of cells expressing CD69 (a), CD25 (b), or incorporating BrdU (c). BrdU incorporation was normalized against the maximum percent cells positive for BrdU in each experiment and is therefore expressed as the relative percent BrdU positive cells.

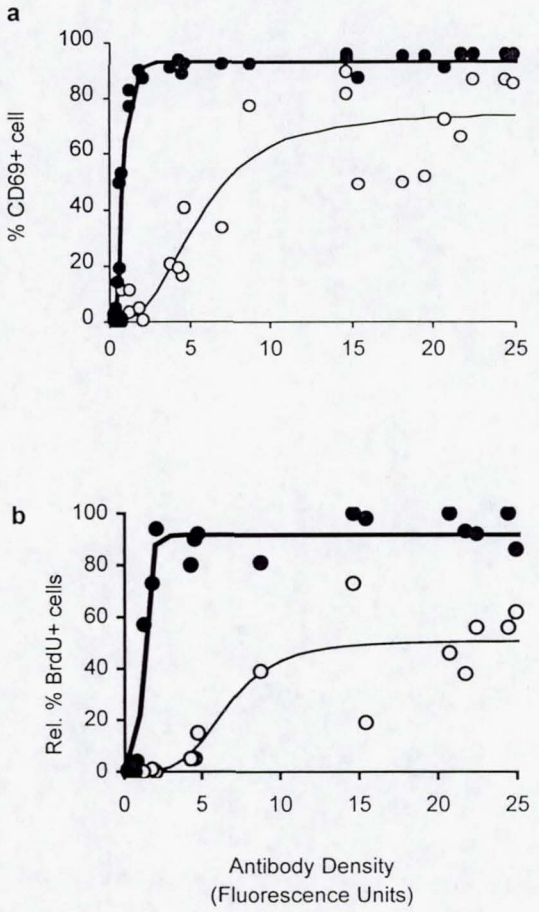

Figure 2 **Curve fit analysis of T lymphocyte activation during clinorotation and static culture**. Least squares curve fit analysis was performed on cumulative data collected during clinorotation (open circles) and static culture (closed circles) using the equation $\%A = \%A_{max}[x^p/((x_{50})^p + x^p]$, where x is the density of anti-CD3/28 in units (measured by indirect immunofluorescence) used for stimulation and %A is the percentage of cells positive for CD69 (a) or relative BrdU incorporation (c). Data is cumulative for 3 (c), or 4 (a,b) independent experiments. Curve fits for clinorotation (thin line) and static culture (bold line) are shown. Equation parameters and statistical values for the curves are given in Table 1.

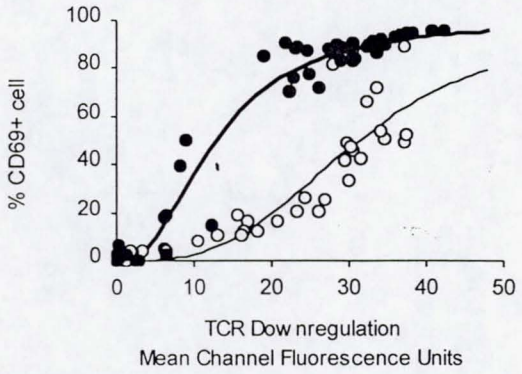

Figure 3 **Activation vs. TCR internalization** The percentage of cells activated (CD69 positive) during clinorotation (open circles) or static culture (closed circles) is plotted as a function of TCR downregulation. TCR downregulation is estimated as the difference in CD3 surface expression, measured by indirect immunofluorescence, between activated and non-activated cells. Data is cumulative for seven independent experiments. Least squares curve fit analysis was performed using the equation $\%A = \%A_{max}[x^p/((x_{50})^p + x^p]$, where x is extent of TCR downregulation (units) and %A is the percentage of CD69 positive cells. Equation parameters and statistical values for the curves are given in Table 1.

	$\%A_{max}$	X_{50}	p	R^2
Fig 2				
CD69				
static	93.00 ± 2.00	0.83 ± 0.04	4.39 ± 0.81	0.9898
clino	74.96 ± 5.90	5.67 ± 0.80	2.82 ± 1.07	0.9441
BrdU				
static	91.70 ± 1.83	1.21 ± 0.05	6.08 ± 1.27	0.9933
clino	50.72 ± 4.53	6.62 ± 1.28	4.16 ± 2.20	0.9099
Fig 3				
69vs3				
static	100.70 ± 6.31	12.84 ± 1.24	2.35 ± 0.40	0.9890
clino	(100)	31.22 ± 0.95	3.17 ± 0.46	0.9114

Table 1 **Curve fit parameters for T cell activation during clinorotation and static culture.** A least squares fit analysis was performed on cumulative data using the equation $\% = \%A_{max}[x^p/((x_{50})^p + x^p]$, where %A is the percentage of cells positive for CD69 or relative BrdU incorporation, and x is the anti-CD3/28 density used for stimulation (units, Fig 2) or the estimated TCR downregulation (units, Fig 3). Empirical values (± sem) determined by the equation and statistical correlations (R-squared values) are shown. Parentheses indicate values not determined empirically by the equation.

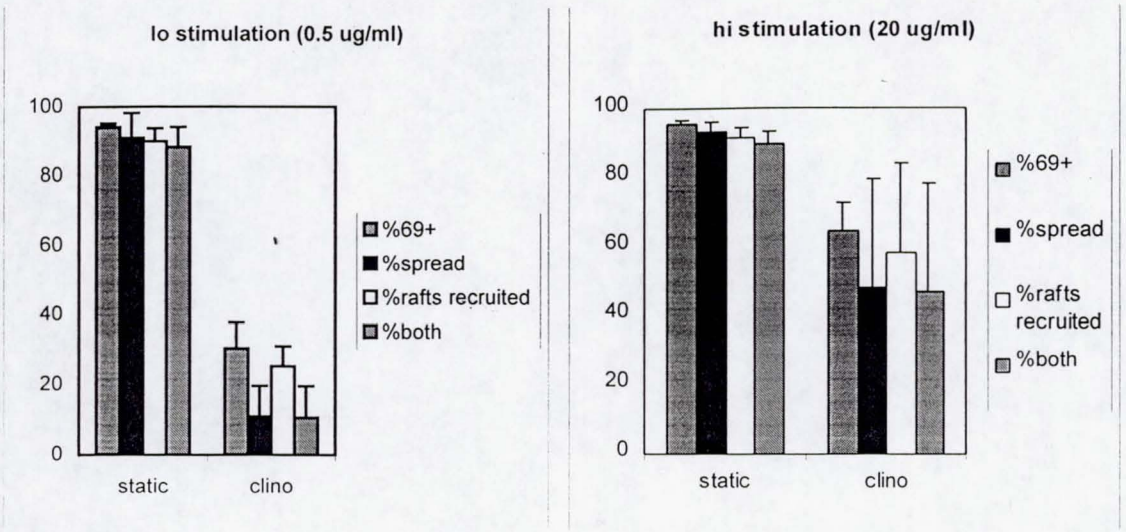

Figure 4 **Activation, cell spreading, and raft recruitment** T cells were analyzed for lipid raft recruitment and cell spreading onto latex beads coated with lo (0.5 ug/ml, 7.0 ± 0.45 units) or hi (20 ug/ml, 30 ± 1.91 units) densities of anti-CD3/28 during clinorotation or static culture (1 hour activation). Lipid rafts were visualized with CTB-FITC (8ug/ml, Sigma). 100 cell/bead interactions were scored for cell spreading (black bars) raft recruitment (open bars), or both (hatched bars) by fluorescent microscopy. CD69 expression (gray bars) was determined at 48 hours for cells activated in parallel. Bars represent the average of three separate experiments (± sem).

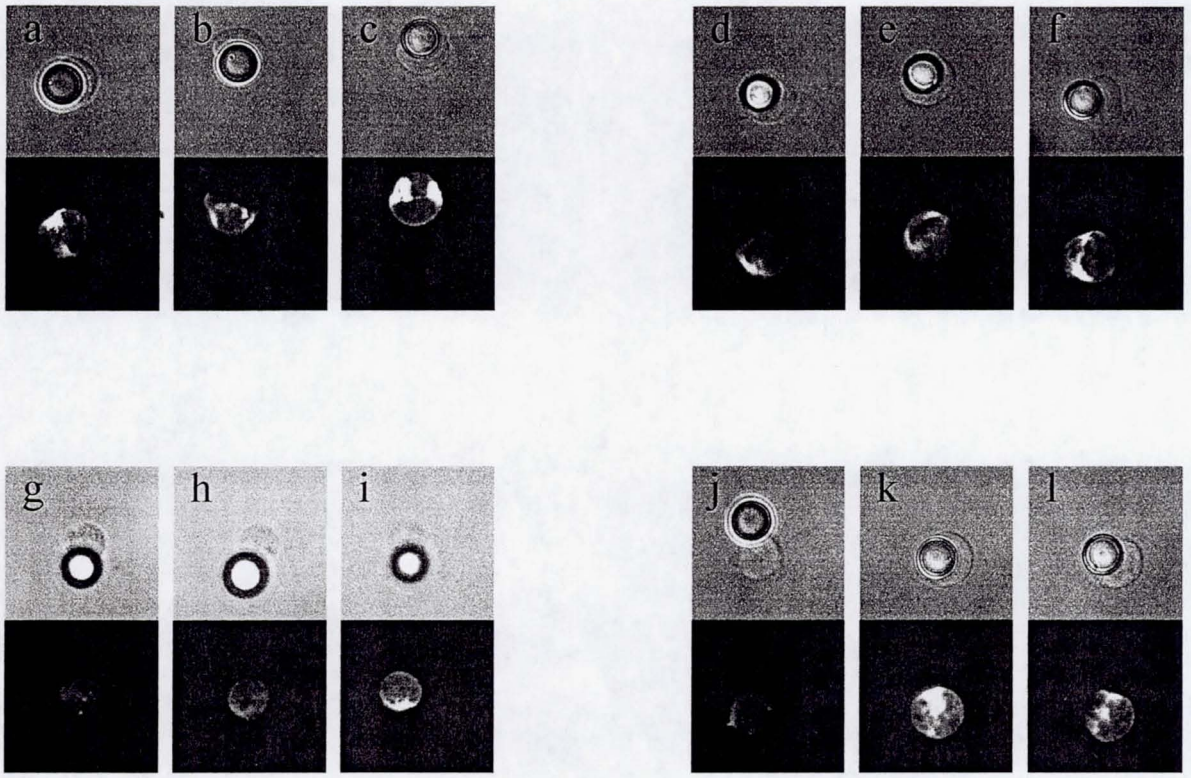

Figure 5 **Confocal image analysis of cell spreading and lipid raft recruitment.** Images represent typical bead/cell interactions for each activation condition. Resting T cells stimulated in static culture with either lo (a-c) or hi (d-f) density of anti-CD3/28 bound to polystyrene beads show dramatic cell rounding around the bead with intense immunolocalization of lipid rafts at the contact site. Cells stimulated with lo anti-CD3/28 during clinorotation (g-i) fail to wrap around the bead. Some cells show raft recruitment in the absence of cell spreading (i), but most do not show raft localization to the contact site (g,h). Cells stimulated with hi anti-CD3/28 during clinorotation (j-l) do spread onto the bead and recruit rafts to the contact site (k,l), but not at the same frequency as cells activated in static culture.